8.3 CLOUD AND PRECIPITATION PROCESSES IN THE 1-2 FEBRUARY 2001 STORM STUDIED OFF THE WASHINGTON COAST IN IMPROVE

Amanda G. Evans, John D. Locatelli, Mark T. Stoelinga, and Peter V. Hobbs*
University of Washington, Seattle, Washington

1. INTRODUCTION

The offshore field phase of the IMPROVE project took place from 4 January – 14 February 2001 off the coast of Washington State. The focus of the data collection was the isolation of frontal forcing as a precipitation generating mechanism in cyclonic storms. A comprehensive set of in-situ and remotely sensed measurements of meteorological state variables and cloud microphysical variables were collected to quantify cloud and precipitation microphysical processes.

This paper focuses on data collected during the passage of an occluding frontal system and associated upper-level, cold-frontal rainbands on 1 February 2001. We will present a synoptic analysis of this storm, describe several of the observed mesoscale features, and discuss the cloud microphysical data and precipitation producing mechanisms.

2. OBSERVATIONAL FACILITIES

The NCAR S-Band, dual-polarized "S-Pol" radar was located in Westport, Washington, where it had an unobstructed view of the offshore study area (Fig. 1). This radar was used for weather surveillance and short-term forecasting; it depicted mesoscale structures and the evolution of precipitation features; polarimetric capabilities provided information on particle types and rainfall rate; and, three-dimensional wind fields were derived from the Doppler measurements provided by two bistatic receivers.

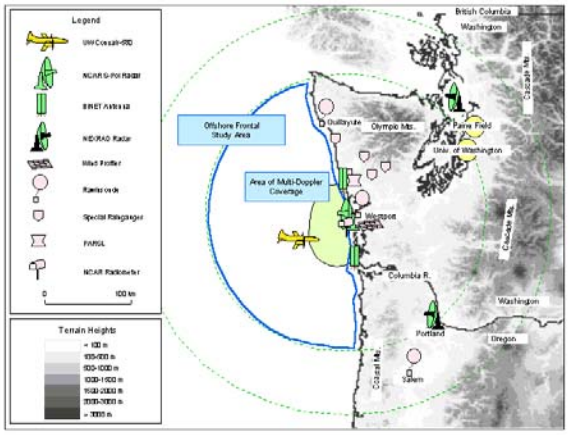

Fig. 1. Schematic of the observational facilities for the offshore phase of the IMPROVE field study.

The University of Washington's (UW) Convair-580 research aircraft collected in-situ measurements of state variables and cloud microphysical variables. Vertically-stacked horizontal flight legs were flown through rainbands to produce vertical cross-sections of recorded microphysical parameters. In the 1 February 2001 case, the flight path corresponded to the 250° azimuth from the Doppler radar, allowing the superposition of the flight track over a vertical cross-sectional scan by the radar.

Special rawinsondes were launched by the National Weather Service at Quillayute, Washington and by the UW from Westport. Other instrumentation and observational facilities included a wind profiler at Westport and rain gauges along the Washington Coast.

3. SYNOPTIC ANALYSIS

On 1 February 2001 an occluding frontal system approached the coast of the Pacific Northwest. Infrared satellite imagery taken at

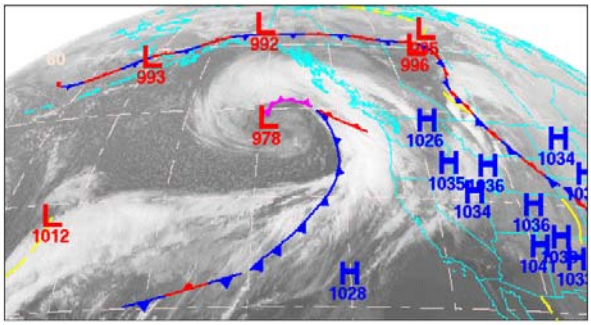

Fig. 2. Infrared satellite image, with NCEP analyzed fronts superimposed, for 0000 UTC 2 February 2001.

**Corresponding author address*: Peter V. Hobbs, Univ. of Washington, Dept. of Atmospheric Sciences, Seattle, WA 98195-1640; e-mail: phobbs@atmos.washington.edu

0000 UTC 2 February 2001 shows a classic comma-shaped cloud and cold-air advection occurring behind the NCEP analyzed cold front (Fig. 2).

A time-height vertical cross-section derived from rawinsonde and wind profiler data is seen in Fig. 3. The tipped-forward structure of the upper-level cold front is clearly visible. The nose of the upper-level cold front corresponds to a surface wind shift, a slight rise in surface pressure at Westport, and the beginning of the precipitation event studied here.

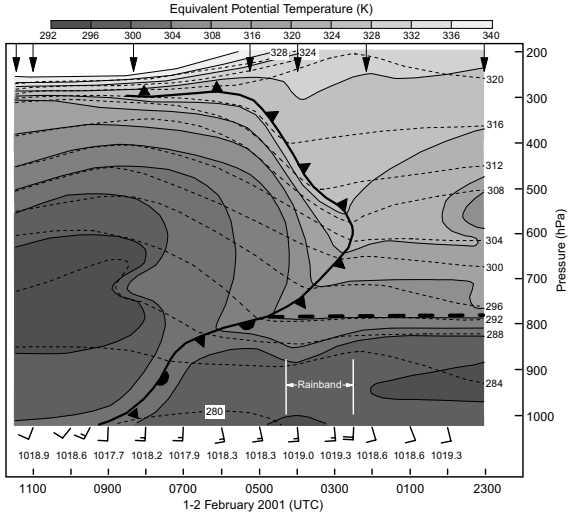

Fig. 3. Time-height cross-section, based on rawinsondes launched from Quillayute and Westport, Washington. Surface winds and pressure (in hPa) are based on in-situ measurements from Westport. Shading indicates various ranges of equivalent potential temperature (θ_e). Lines of constant potential temperature are labeled in K.

The main rainband in which the Convair-580 collected data was associated with the upper-level cold front seen in Fig. 4. An overlay of radar reflectivity from the Westport site, and a composite of NWS radar reflectivity data indicates the coincidence of the upper-level front with the main rainband.

4. MESOSCALE FEATURES

Within the main rainband, shown in Fig. 4, were smaller bands of intense precipitation, as seen in the radar reflectivity values shown in Fig. 5a. These smaller precipitation bands will be referred to as *sub-bands*. The sub-bands were oriented in a northwest-southeast direction and were approximately 30 km apart. While the main rainband moved with a velocity of 12 m s^{-1}, the sub-bands moved with a velocity of 17 m s^{-1}. The sub-bands are still clearly visible in the higher radar elevation angle scan (2.3°) shown in Fig. 5b, even in areas where no precipitation reached the ground. This indicates that the sub-bands were generated somewhere between 3 and 6 km.

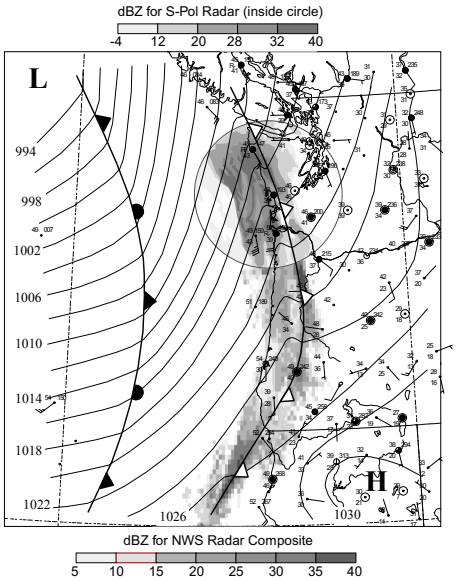

Fig. 4. Synoptic map for 0300 UTC 2 February 2001. Isobars are labeled in hPa. Surface and upper-level fronts are indicated in the conventional manner. Precipitation intensity, measured by the NCAR S-Pol radar at Westport and NWS radars at Portland and Medford, Oregon, and Eureka, California, are shown by shading.

To investigate the generation of the sub-bands, we examined areas of more intense precipitation (i.e., *precipitation cores*). Precipitation cores were tracked over a series of radar scans and were found to move from a direction of 188° to 208° and speeds of 27 to 30 m s^{-1}. Comparison with the soundings shows that the motions of the precipitation cores corresponded to the wind speed and direction in a vertical layer from 2 to 7 km.

Vertical cross-sectional scans from the S-Pol radar show two layers of *generating cells* (Figs. 6a and 6b). The layer located between 9 and 10 km will be referred to as the *cirrus generating cells*, and the layer between 5 and 7 km as the *altocumulus generating cells*. The radar reflectivity was approximately 20 dB greater in the fall-streaks from the latter generating cells. Therefore, we conclude that the precipitation cores were produced by the altocumulus generating cells.

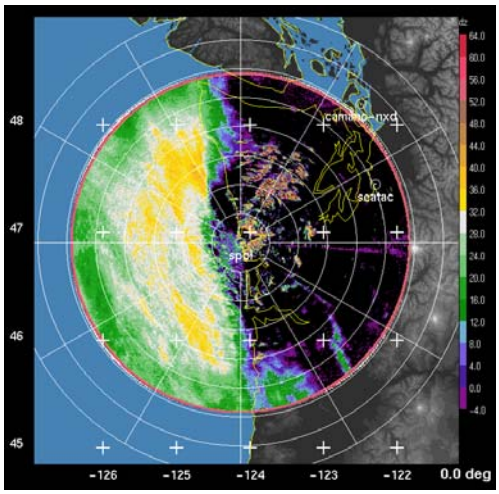

(a)

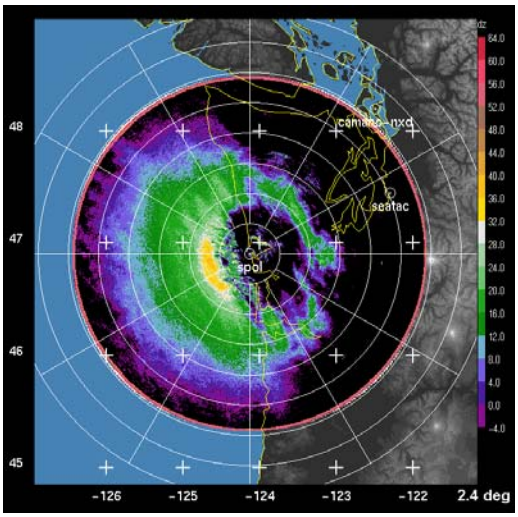

(b)

Fig. 5. PPI radar reflectivity factor patterns measured by the NCAR S-Pol radar at Westport, Washington, on 2 February 2001 at (a) 01:36:46 UTC at 0.5° elevation scan and (b) 01:38:39 UTC at 2.4° elevation scan.

Previous research has shown that contributions to precipitation mass by generating cells ranges from 20-35% (Hobbs et al. 1980, Houze et al. 1981) depending on the strength of the vertical air motions within the cells. Earlier model simulations (Rutledge and Hobbs, 1983) artificially inserted the effects of generating cells. In future studies, we will investigate if mesoscale models can replicate the role of generating cells, or if the cells need to be parameterized.

5. ICE CRYSTAL ANALYSIS

Ice crystal types can provide important information including the identification of the temperature zones for precipitation growth, particle growth mechanisms, regions of water and subwater saturation, and the fall speeds of crystals. The primary instrument for ice crystal identification in the 1 February 2001 case was the Cloud Particle Imager (CPI). The CPI uses a pulsed laser to produce detailed 2-D images of cloud particles down to 10 μm in size. Examples of these images and the temperatures and saturations where they formed are given in Fig. 7.

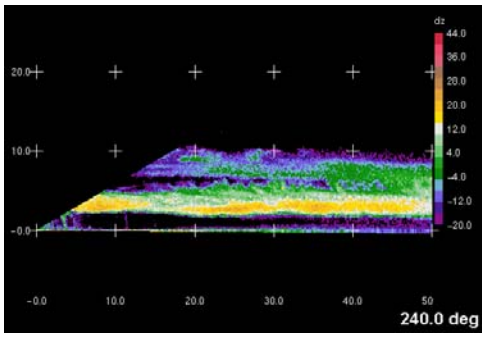

(a)

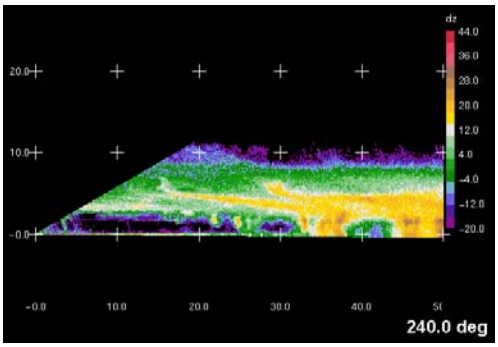

(b)

Fig. 6. RHI radar reflectivity factor patterns measured by the NCAR S-Pol radar at Westport on 2 February 2001 at (a) 00:54:01 UTC at 240.0° azimuth from radar and (b) 01:25:02 UTC at 240.0° azimuth from radar.

Over 99,000 crystal images were analyzed to determine the dominant crystal types and degrees of riming for each minute of the flight. This analysis confirmed that each crystal type had a well-defined formation temperature (Fig. 8). It can also be seen from Fig. 8 that the altocumulus generating cell region corresponds to the temperature zone in which sideplanes and assemblages of

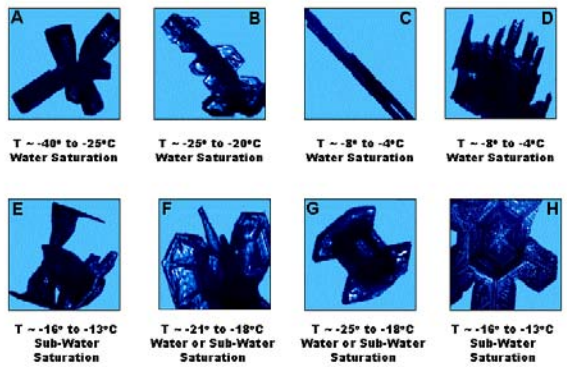

Fig. 7. Some crystal types recorded by the Cloud Particle Imager (CPI) on 1-2 February 2001. (A) assemblage of bullets, (B) sideplanes, (C) sheaths, (D) plate with sheaths growing from face, (E) capped assemblage of bullets, (F) radiating assemblage of plates, (G) capped column, and (H) broad-branched crystal. Corresponding temperatures and saturation conditions for the formation of the crystals are noted.

plates formed, while bullets and plates most likely formed in the cirrus generating cell region. In the dendritic region, where we expect to see the most vigorous crystal growth under water saturated conditions, only a few broad-branched and sector-like crystals, which form in sub-water saturated conditions, were observed. No dendrites were seen. Very little growth of ice particles by riming was observed in this storm, unlike the case study of orographic precipitation described by Woods et al. (2003).

Work is currently underway to determine mass mixing ratios and fall speeds of ice particles along the flight track. This information will be used to determine the vertical velocities within the alto-cumulus generating cells and precipitation rates along the flight track, which will be compared with precipitation rates derived from the Doppler radar and mesoscale model outputs.

6. SUMMARY

The occluding cyclone studied off the Pacific Coast on 1 February 2001 is typical of those that make landfall in the Pacific Northwest in winter. Preliminary analyses of a comprehensive data set for this cyclone, collected in the IMPROVE study, shows the main rainband was associated with the upper-level cold front. Within this rainband were several sub-bands of more intense precipitation that originated in altocumulus generating cells. Sideplanes and assemblages of plates, which form at water or sub-water saturation, were the pri-

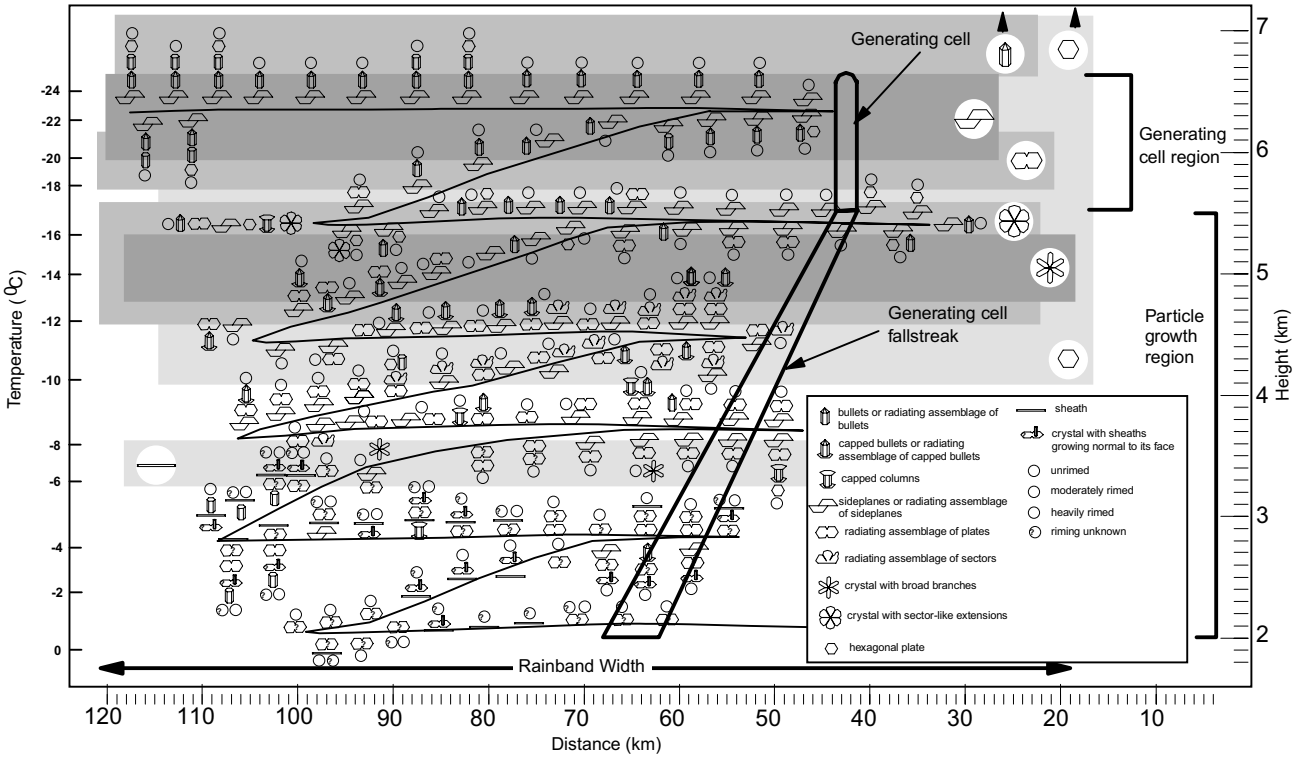

Fig. 8. Vertical cross-section of storm-relative flight track with dominant crystal types identified for each minute of flight. The crystals that grow in the various temperature zones are indicated.

mary ice crystals formed in these generating cells.

Future work will be done to determine how the synoptic-scale features affected the generating cell structure, their effect on cloud microphysics, and the ability of mesoscale models to replicate these features. We will also complete the analysis of the Doppler-derived wind field and Convair data, including liquid water content, particle size spectra, and particle type, for comparison with mesoscale model outputs.

7. ACKNOWLEDGEMENTS

Research supported by grant ATM-9632580 from the Mesoscale Dynamic Meteorology Program, Atmospheric Sciences Division, NSF.

8. REFERENCES

Hobbs, P.V., T.J. Matejka, P.H. Herzegh, J.D. Locatelli, and R.A. Houze Jr., 1980: The mesoscale and microscale structure and organization of clouds and precipitation in midlatitude cyclones. I: A case study of a cold front. *J. Atmos. Sci.*, **37**, 568-596.

Houze, R.A., Jr., S.A. Rutledge, T.J. Matejka, and P.V. Hobbs, 1981: The mesoscale and microscale structure and organization of clouds and precipitation in midlatitude cyclones. III: Air motions and precipitation growth in a warm-frontal rainband. *J. Atmos. Sci.*, **38**, 639-649.

Rutledge, S.A., and P.V. Hobbs, 1983: The mesoscale and microscale structure and organization of clouds and precipitation in midlatitude cyclones. VIII: A model for the feeder-seeder process in warm-frontal rainbands. *J. Atmos. Sci.*, **40**, 1185-1206.

Woods, C.P., M.T. Stoelinga, J.D. Locatelli, P.V. Hobbs, 2003: Cloud and precipitation processes observed in the 13-14 December 2001 storm studied over the Oregon Cascades in IMPROVE. *10th Conference on Mesoscale Processes,* Portland, OR, Amer. Meteor. Soc., this issue.